Complex Systems **6** (1992) 137–161

Quantum Chaos on Hyperbolic Manifolds: A New Approach to Cosmology

Roman Tomaschitz
Dipartimento di Matematica Pura ed Applicata
dell' Università degli Studi di Padova,
Via Belzoni 7, I-35131 Padova, Italy
and
Instituts Internationaux de Physique et de Chimie Solvay
Université Libre de Bruxelles,
C.P. 231–Campus Plaine, Bd. du Triomphe,
B-1050 Brussels, Belgium

Abstract. We consider classical and quantum motion on multiply connected hyperbolic spaces, which appear as space-like slices in Robertson-Walker cosmologies. The topological structure of these manifolds creates on the one hand bounded chaotic trajectories, and on the other hand quantal bound states whose wave functions can be reconstructed from the chaotic geodesics. We obtain an exact relation between a probabilistic quantum mechanical wave field and the corresponding classical system, which is likewise probabilistic because of the instabilities of the trajectories with respect to the initial conditions. The central part in this reconstruction is played by the fractal limit set of the covering group of the manifold. This limit set determines the bounded chaotic trajectories on the manifold. Its Hausdorff measure and dimension determine the wave function of the quantum mechanical bound state for geodesic motion.

We investigate relativistic scalar wave fields in de Sitter cosmologies, coupled to the curvature scalar of the manifold. We study the influence of the topological structure of space-time on their time evolution. Likewise we calculate the time asymptotics of their energies in the early and late stages of the cosmic expansion.While in the late stages both bounded and unbounded states approach the same rest energy, they show significantly different behavior at the beginning of the expansion. While the stable bound states have simple power law behavior, extended states show oscillations in their energy, with a frequency and an amplitude both diverging to infinity, indicating the instability of the quantum field at the beginning of the cosmic expansion.

1. Introduction

Little else has led to as much controversy in twentieth-century physics as the question about the probabilistic or deterministic nature of the microscopic laws of motion. The problem is that, despite the complete failure of classical mechanics applied to microscopic problems and the universal success of quantum mechanics as a tool of prediction and calculation, the questions why quantum mechanics works and which structures we really calculate with it are not answered by the probabilistic interpretation of ψ, Schrödinger's wave function.

In this work we present a simple example, geodesic motion on multiply connected Riemannian spaces of constant negative curvature and infinite volume, and reconstruct wave functions from chaotic classical trajectories in an exact, non-semiclassical way.

It might seem strange that it is possible to reconstruct a non-deterministic wave field from classical geodesics. The point here is that we actually relate two probabilistic models of microscopic motion, that of quantum mechanics and that of unstable classical dynamics. The classical trajectories in question have positive Lyapunov exponents, and the exponential divergence of initially neighboring trajectories makes it impossible to determine their evolution using Newton's equations, given the finite accuracy of the initial conditions. These equations are true at every moment of the motion, but not as an initial value problem predicting the future. They are just an expression of the following insight, Newton's (second) law: "The change in motion is proportional to the motive force impressed and occurs along the right line in which that force is impressed."[1]

The scenario here is that the particles, if their motion is bounded, inhabit a finite domain of the manifold, and their trajectories there are dense, ergodic, and mixing. Thus a classical point particle is, despite the fact that it moves along a smooth trajectory, after a short Lyapunov time not any more localizable within this domain (this domain is one and the same for all bounded trajectories).

In quantum mechanics we have the fundamental principle that the initial values, say of momentum and coordinates, cannot be realized simultaneously with arbitrary precision due to uncertainty relations. In classical but unstable mechanics it is true that we can prepare the initial values of the coordinates and the momentum with any wished finite precision, but the inevitable error augments exponentially after the Lyapunov time. In particular, if we choose a Gaussian initial distribution for the momentum and the coordinates, and apply the geodesic flow to it, we observe dispersion of the classical probability density. Moreover in the dynamical system that we consider here, namely geodesic motion on negatively curved spaces, the classical probability density

[1] *Mutationem motus proportionalem esse vi motrici impressae et fieri secundum lineam rectam qua vis illa imprimitur.* Cited from I. B. Cohen, *Introduction to Newton's Principia* (Cambridge, MA, Harvard University Press, 1971).

disperses at the same rate as the quantum mechanical one, if we start with the same initial distribution. Thus in both cases, though the reasons are quite different, the particle slips through our attempts to predict its future.

In section 2 we give a sketch of classical non-relativistic mechanics on hyperbolic 3-manifolds. In section 3 we perform the above-mentioned reconstruction. We embed the manifold into its universal covering space; the ground state wave function is then completely determined by the limit set of the covering group (namely by the Hausdorff measure and the Hausdorff dimension of this singular set). On the other hand, this limit set emerges as the set of initial and end points of the bounded trajectories lifted into the covering space. In section 4 we discuss the analytic construction of these singular sets, which provide the basic link between the chaotic trajectories and the bound state wave functions, and give some numerical examples.

In section 5 we apply this formalism to relativistic wave fields in Robertson-Walker cosmologies. This needs some introductory comments. Cosmologies satisfying the principle of homogeneity and isotropy are described by a four-dimensional Riemannian space, whose space-like slices—namely the three-dimensional sections at a fixed time—are 3-manifolds of constant Gaussian curvature. Einstein's equations do not determine the topological structure of these sections, and usually the topology is assumed to be trivial, given either by flat Euclidean space or the 3-sphere in the case of positive curvature (closed model, finite volume), or by a shell of the three-dimensional Minkowski hyperboloid in the case of negative curvature (open model, infinite volume). This is so partially for reasons of simplicity, and partially because of lack of observational evidence, given that even the question of whether the universe is closed or open is nowadays far from being resolved.

Soon after Einstein had proposed his cylindrical universe, the mathematician Felix Klein, well aware of Poincaré's work on 3-manifolds and fundamental polyhedra, pointed out that the 3-sphere representing the 3-sections in this model may also be regarded topologically as projective space, if one identifies diametrically opposite points [5]. Since then the possibility of a non-trivial topological structure has been apparent, and has been mentioned from time to time (see [8, 13]).

Cosmologies locally described by a Robertson-Walker line element are regarded today as the most likely candidates to provide realistic models for the evolution of the universe, and in [18] we started to investigate the influence of the possible multiple connectivity of the space-like slices on the dynamics of particles geodesically moving on them. How does the topology influence the dynamics, and can one draw from the dynamics of particles conclusions about the topology? This approach is in some sense reminiscent of Mach's principle, namely that the global structure of the universe determines the local laws of motion—inertial forces being gravitational—stemming from the mass content of the whole (closed) universe. But our emphasis lies more on the topological structure of the open universe, which is in turn related to the energy momentum tensor of the mass distribution.

In section 5 we also investigate wave solutions of the Klein-Gordon equation in de Sitter space. Such solutions are characterized by three parameters: mass; the dimensionless coupling constant of the field to the curvature scalar; and the spectral variable of the Laplace-Beltrami operator of the space-like slices, which are now multiply connected and open. The non-minimal coupling of the field to the curvature is essential for the treatment of massless particles.

We find bound states of wave fields and the corresponding chaotic trajectories that are both foreign to the traditional open models in cosmology. Finally we calculate the time evolution of the energy of wave fields in the early and late stages of expanding de Sitter space. While in the late stages, when 3-space gets asymptotically flat and the energy always approaches essentially the classical rest energy, we find crucial qualitative differences in the evolution of bound states and extended states at the beginning of the cosmic evolution. Oscillations appear in the energies of the extended states whereas the bound states show simple power law behavior, the exponents being determined by the Hausdorff dimensions of the limit sets of the covering groups of the space-like slices; for further discussion we refer to the conclusion, section 6.

2. A short précis on classical mechanics in hyperbolic spaces

Three-dimensional hyperbolic space H^3, a shell of the Minkowski hyperboloid $x_0^2 - \mathbf{x}^2 = R^2$ and endowed with the metric $ds^2 = d\mathbf{x}^2 - dx_0^2$, can be isometrically represented as an open ball B^3, $|\mathbf{x}| < R$, with the metric

$$d\sigma^2 = 4(1 - |\mathbf{x}|^2/R^2)^{-2} d\mathbf{x}^2, \tag{2.1}$$

which induces constant negative sectional curvature $-1/R^2$ on B^3. For details in this section we refer to [2, 11, 17].

Geodesics in this geometry are arcs of circles orthogonal to S_∞ ($|\mathbf{x}| = R$, the sphere at infinity of hyperbolic space), and the geodesic planes are domains on spherical caps orthogonal to S_∞.

A hyperbolic manifold, that is, a manifold of constant negative curvature, can be embedded in B^3 as a non-Euclidean polyhedron whose faces (lying on geodesic planes) are identified in pairs with elements of the invariance group of the metric, the Lorentz group $SO^+(3,1)$. The polyhedron may also have free faces, domains on S_∞ that are not identified, representing the boundaries of the manifold at which the conformal factor of the metric gets infinite.

Arp's sculpture in figure 1 is an example of how such a hyperbolic manifold may look if the identification of the polyhedral faces is carried out. It is a surface of finite thickness, a topological product $I \times S$ of a finite open interval and a compact Riemann surface of genus four. If we remove the interior and exterior boundaries—that is, if we take the open interval—we get a complete metric space.

In figure 2 we have drawn the ring of base circles on S_∞ of the spherical caps on which the faces of the polyhedron lie. The exterior domains of the

Fig.1

Figure 1: Jean Arp's sculpture Ptolémée II, 1958, is the typical example for the topological structure of a hyperbolic manifold with the identification pattern in figure 2. The exterior visible boundary corresponds to f_1, the interior surface of the bronze layer to f_2. (Photo by E. B. Weill. Reproduced with permission.)

ring, f_1 and f_2, are the two free faces of the polyhedron, which fill the whole space B^3 with the exception of the interior of the caps.

If we identify the caps in the way indicated in figure 2, we get topologically a thickened surface of genus four, like the bronze sculpture in figure 1. The actual realization of this identification pattern in B^3 has to be chosen so that the metric inherited from B^3 fits smoothly on the identified faces. The criterion for this is that the Kleinian group Γ generated by the face-identifying transformations tesselates if applied to the polyhedron F, the interior of the spherical caps.

Trajectories in the manifold are realized by projecting B^3-geodesics into F: If the circular arc intersects a tile $\gamma(F)$, the arc piece lying in this tile is mapped via γ^{-1} back into F. The set of all projected arc pieces constitutes the trajectory in F, the initial and end points of the arcs being properly identified by the identification of the polyhedral faces.

The group Γ is countably infinite, and therefore the Γ-images of F—which constitute a tiling of B^3—have accumulation points. They lie on S_∞ and constitute the limit set $\Lambda(\Gamma)$, a closed quasi self-similar Jordan curve in the ring of base circles of the caps. Since Γ leaves S_∞ invariant, $\Lambda(\Gamma)$ appears likewise as the set of accumulation points of images of f_1 and f_2, $\Gamma(f_1 \cup f_2) = \Gamma(f_1) \cup \Gamma(f_2)$, where $\Gamma(f_1)$ approximates $\Lambda(\Gamma)$ from the interior of the ring of base circles (see figures 7 and 5 for the manifolds in figures 2 and 3(b)), and $\Gamma(f_2)$ approximates $\Lambda(\Gamma)$ from the exterior. In figures 4 and 6 we show the complete tesselations $\Gamma(f_1) \cup \Gamma(f_2)$ of S_∞ for manifolds corresponding to the identification patterns in figures 3(b) and (a). Different realizations of the same pattern, for example figures 4 and 5 of the pattern in figure 3(b), lead to globally non-isometric manifolds of the same topological structure. The different Hausdorff dimensions (see the figure captions) of curves corresponding to the same pattern reflect this fact, for they are determined by the ground-state energy of the Schrödinger operator, which is in turn completely determined by the global metric structure of the space.

In the non-relativistic case (section 3) we call a trajectory bounded if it lies in a finite domain, such as a sphere of finite hyperbolic radius, during the whole time evolution given by Newton's equations

$$\frac{d\mathbf{v}}{dt} = \frac{1}{R^2}\left[\mathbf{x}\cdot\mathbf{v}^2 - \mathbf{v}\cdot(\mathbf{x}\cdot\mathbf{v})\right], \tag{2.2}$$

where $\mathbf{v} := d\boldsymbol{\sigma}/dt = 2(1-|\mathbf{x}|^2/R^2)^{-1}d\mathbf{x}/dt$. The relativistic concept of boundedness in a time-dependent metric we give in section 5. The bounded trajectories are exactly the projections of B^3-geodesics with initial and end points in $\Lambda(\Gamma)$: applying Γ to a B^3-geodesic (circular arc) with initial and end points in $\Lambda(\Gamma)$, we get countably many such arcs because of the invariance of $\Lambda(\Gamma)$ under Γ. Their intersection with F gives the projected trajectory. The trajectory is bounded because the arc pieces are uniformly separated from S_∞. These projections are just covering projections from the universal cover B^3 into the manifold F. Γ is the group of covering transformations, and F is the quotient $B^3\backslash\Gamma$. The bounded trajectories fill densely a finite domain in

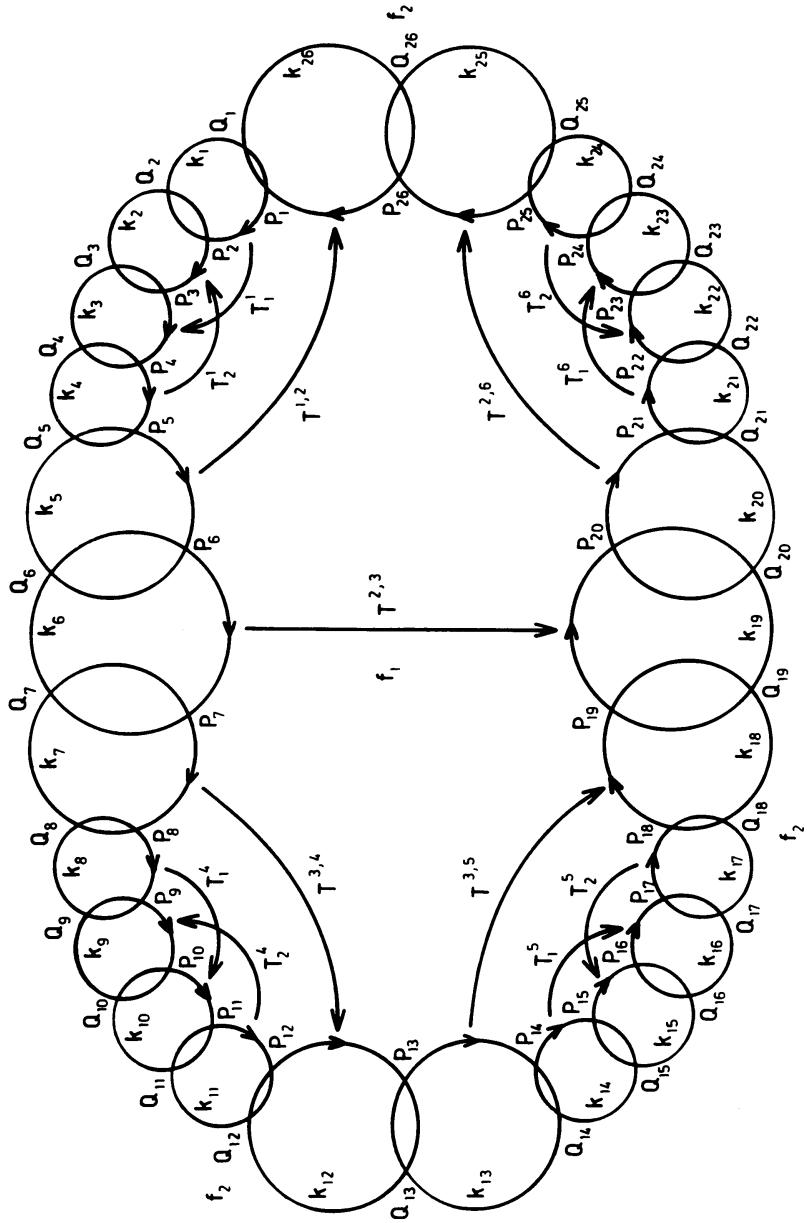

Figure 2: Identification pattern for figure 1. The manifold is embedded in hyperbolic space, the ball B^3, as a non-Euclidean polyhedron. The ring of base circles has to be visualized on S_∞, the boundary of B^3. Spherical caps orthogonal to S_∞ are placed on these circles and identified in the indicated way. f_1 and f_2, the complements of the ring on S_∞, represent compact surfaces of genus four, the two boundary components of the manifold. The identification mappings T are partitioned into cycles (see [11]), satisfying cycle relations like $T^{1,2} \cdot T_2^{1\,-1} \cdot T_1^{1\,-1} \cdot T_2^1 \cdot T_1^1 = \mathrm{id}$, $T^{1,2-1} \cdot T^{2,6} \cdot T^{2,3} = \mathrm{id} \ldots$

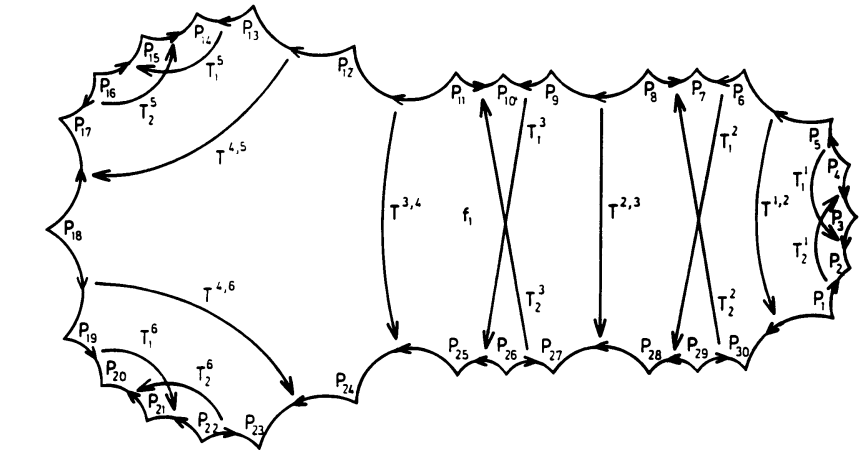

(*a*)

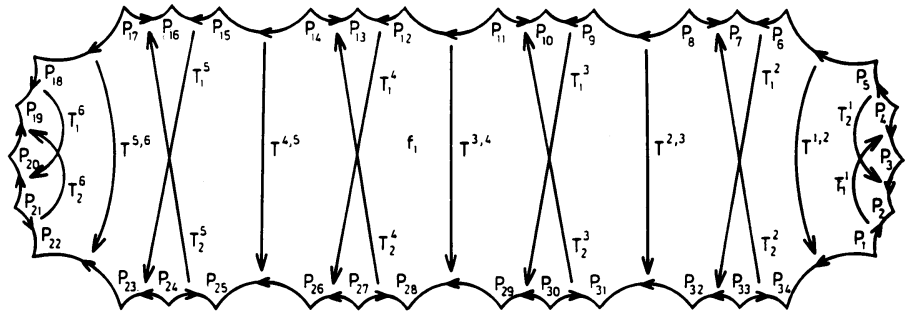

(*b*)

Figure 3: These identification patterns give rise to manifolds similar to that in figure 1, but now of genus five (*a*) and six (*b*). The diagrams have to be completed as in figure 2; as depicted they are the identification patterns of fibers (compact Riemann surfaces) of the manifolds, which fiber over a finite open interval.

F, uniformly separated from S_∞, namely the quotient $C(\Lambda)\backslash\Gamma$, where $C(\Lambda)$ is the hyperbolic convex hull of Λ (see [16]).

If the end point of the arc to be projected does not lie in the limit set, it intersects for $t \to \infty$ only finitely many polyhedra of the tesselation, so the particle approaches one of the boundary surfaces of the manifold (in the projection of the arc in the last intersected polyhedron).

Moreover, from this construction it is also obvious that bounded trajectories can be screened by unbounded ones if we choose their initial and end points sufficiently close to the limit set. Thus, though there are only a few bounded trajectories, many unbounded trajectories will stay arbitrarily long in the manifold before ultimately tending to infinity.

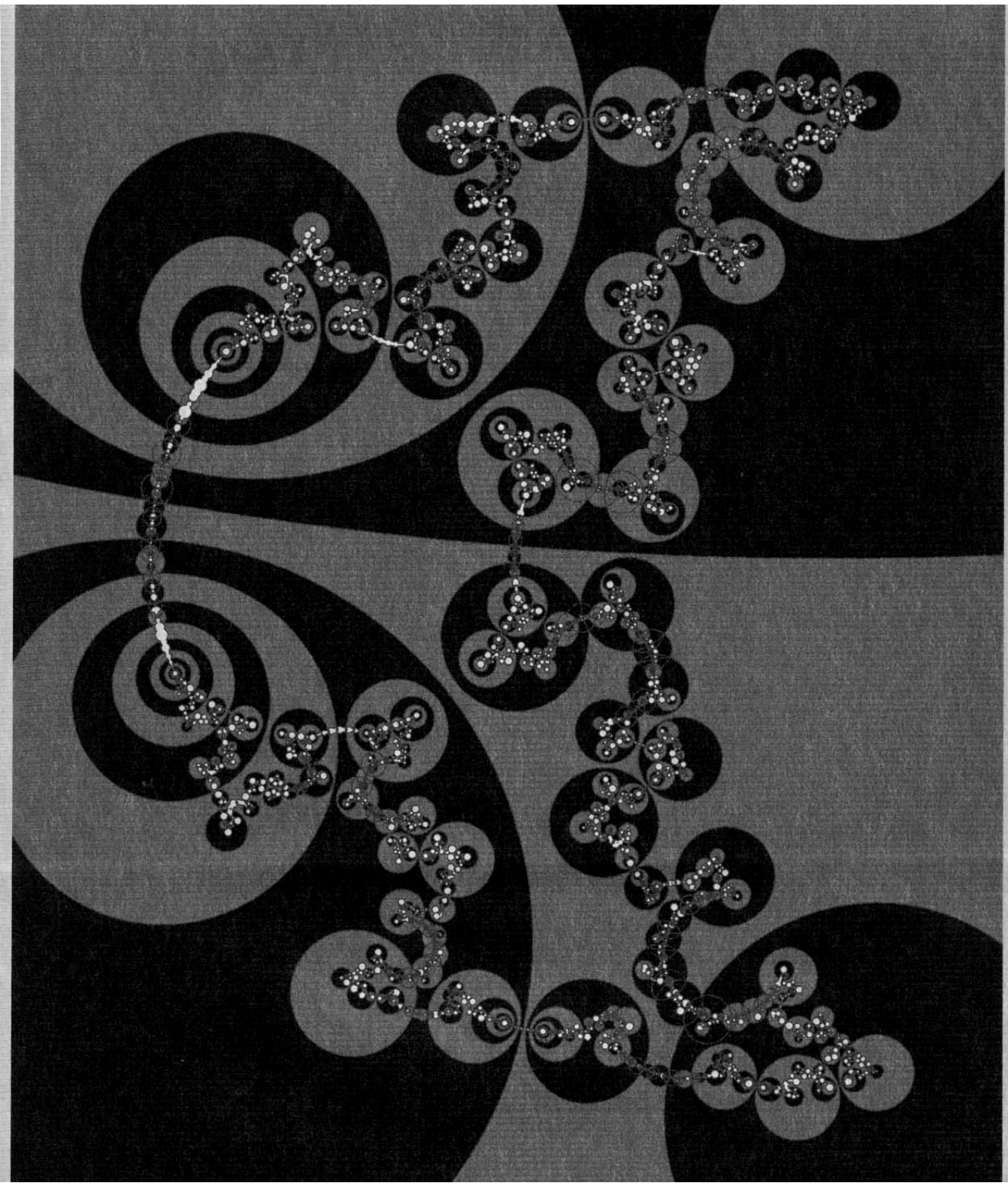

Fig.4

Figure 4: If we apply the discrete group Γ generated by the side-pairing mappings in figure 3(b) to the free polyhedral faces f_1 and f_2, we get a tiling of the interior $\Gamma(f_1)$ and the exterior $\Gamma(f_2)$ of the Jordan curve $\Lambda(\Gamma)$. This curve itself emerges as the set of accumulation points of Γ-images (tiles) of f_1 and f_2. $\Lambda(\Gamma)$ is the support of the Hausdorff measure in the integral representation of the wave function, and constitutes the set of initial and end points of lifts of bounded trajectories. Its Hausdorff dimension δ gives the ground state energy. For the calculation of δ from the tiling see [17]. $\delta = 1.277 \pm 0.001$.

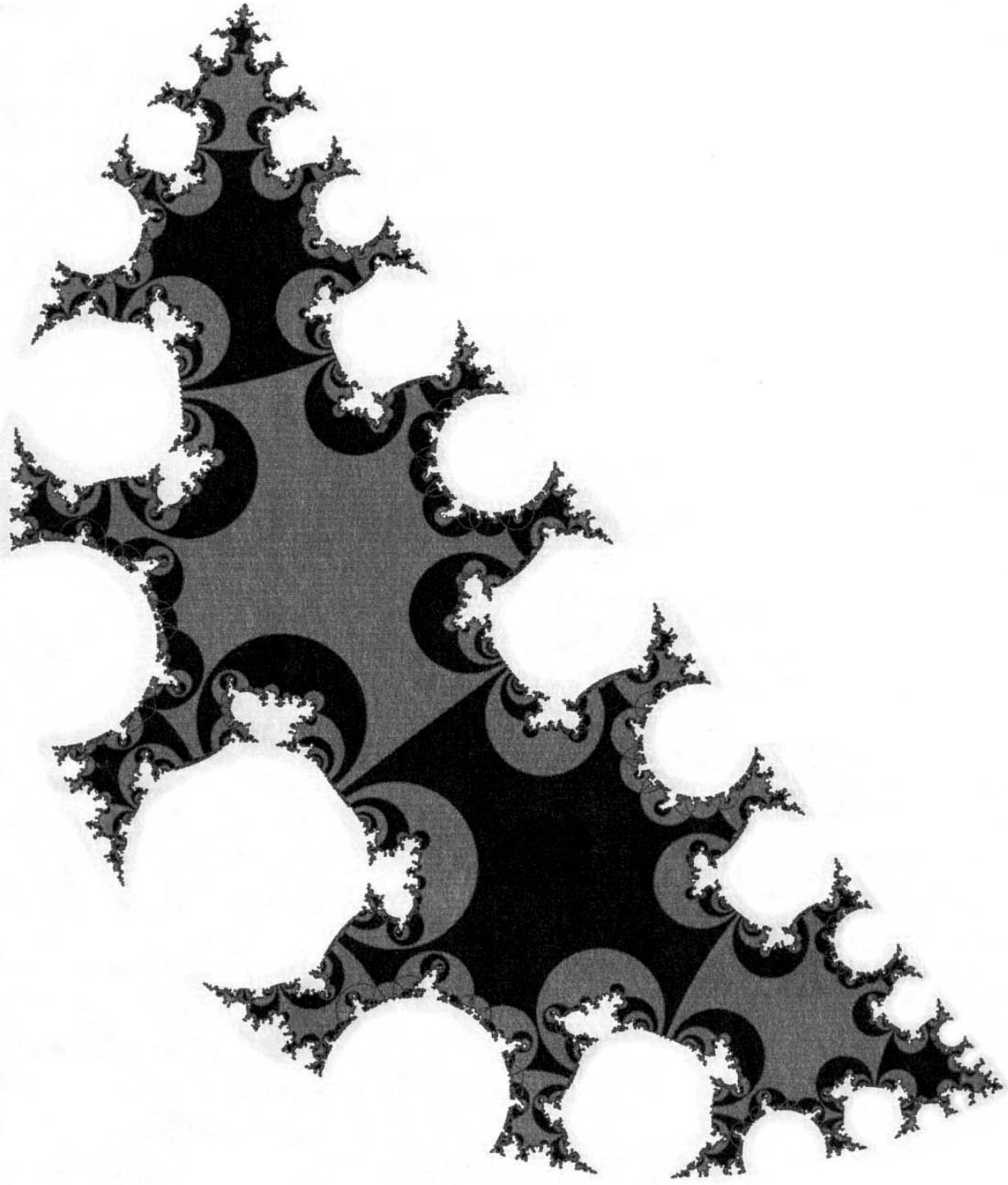

Fig.5

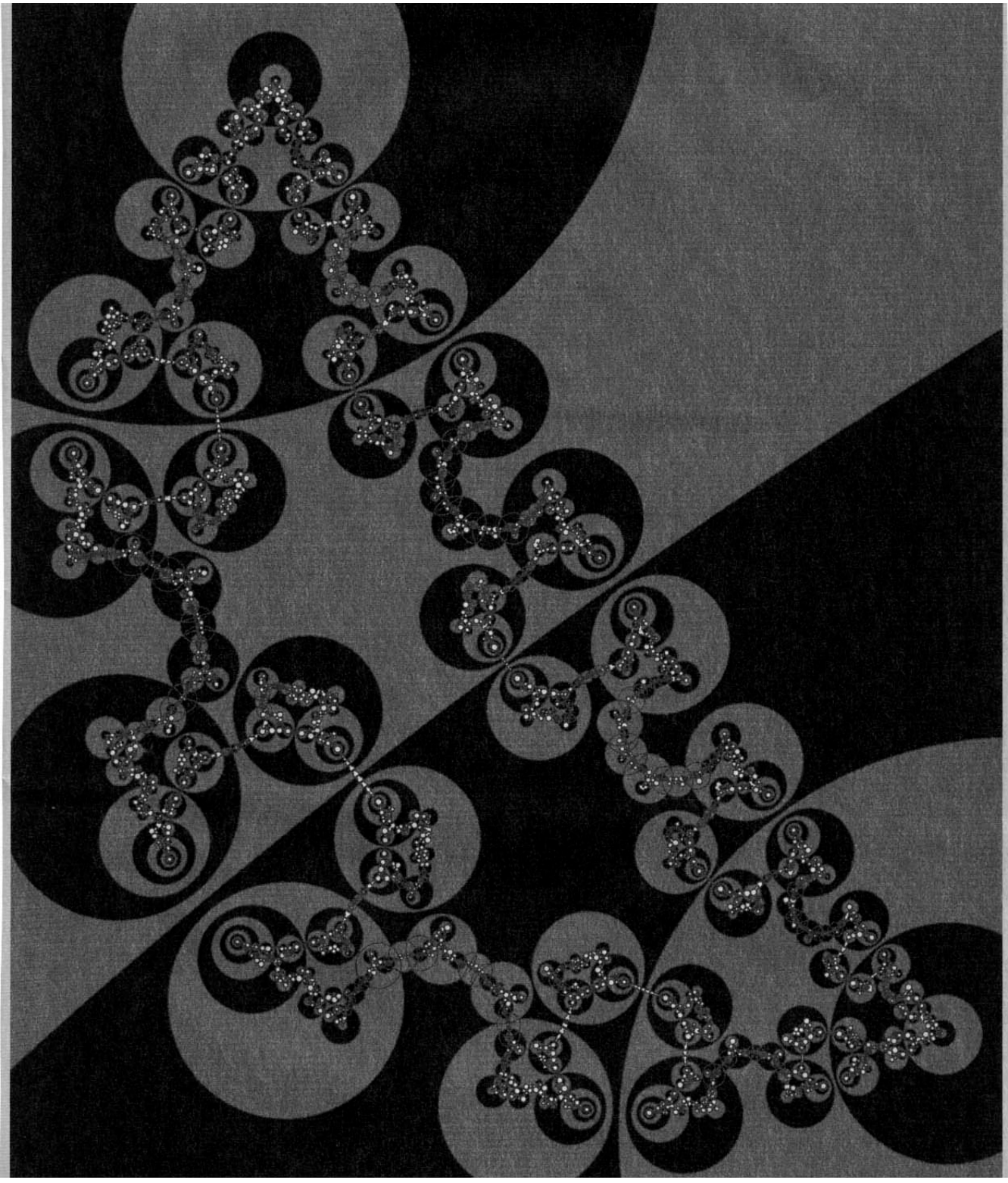

Figure 5: A tesselation corresponding to a manifold with figure 3(b) as an identification pattern; we have drawn $\Gamma(f_1)$, the interior of the Jordan curve. Different realizations (figures 4 and 5) of the same pattern lead to non-isometric manifolds and different limit sets. These fractal sets on the boundary of the universal covering space completely determine both the bounded trajectories and the ground state wave function. $\delta = 1.289$.

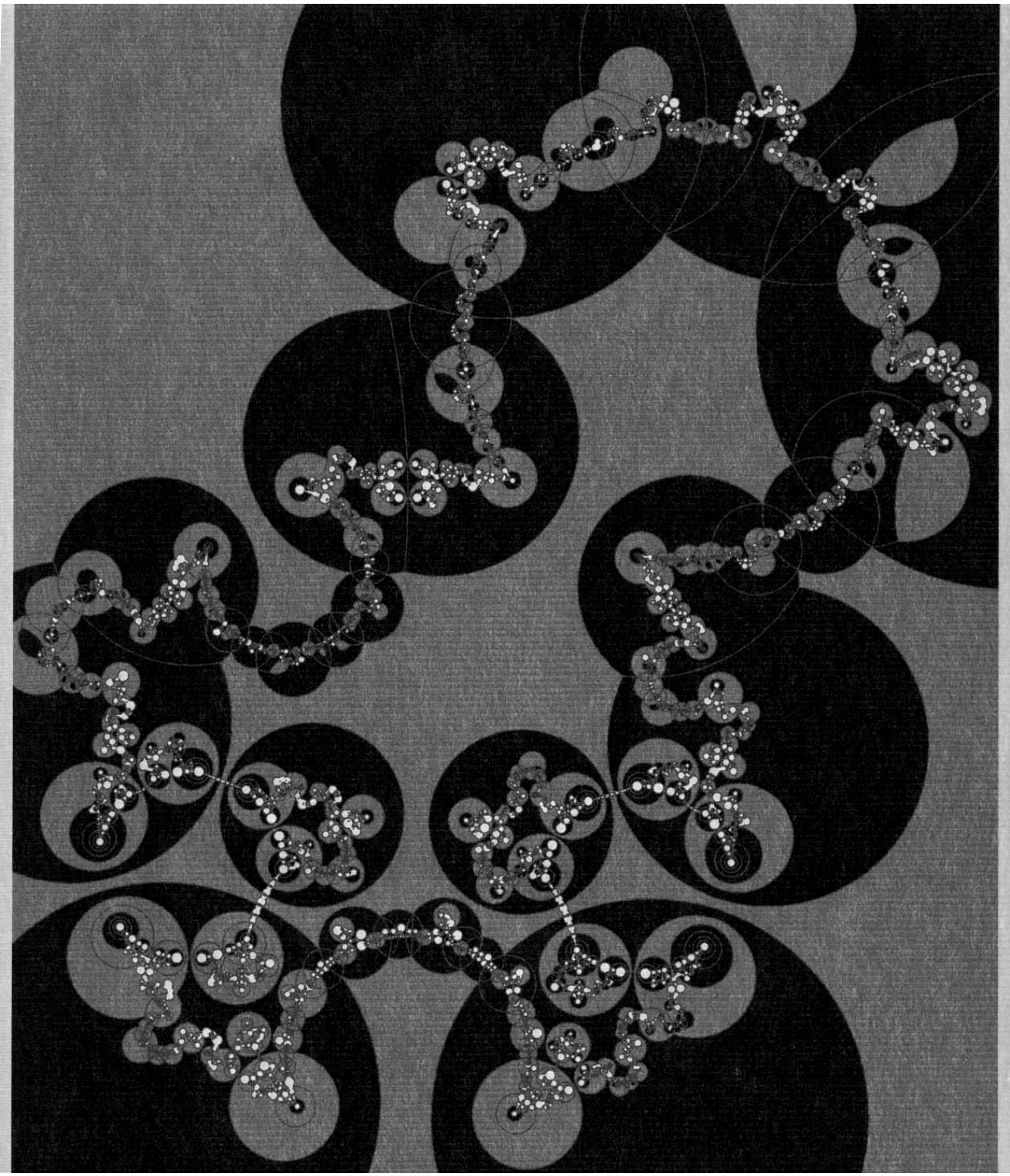

Fig.6

Figure 6: Same as figure 4, but for the pattern in figure 3(a). A quasiconformal, quasi-isometric deformation ω of the unit disk (see section 3) gives rise to this embryonic shape, whose boundary is quasi-self-similar [1]: homothetically magnifying an arbitrarily small piece of the curve, we observe similar shapes (in the sense of a quasi-isometry) as we do on the scale of the whole figure. $\delta = 1.300$.

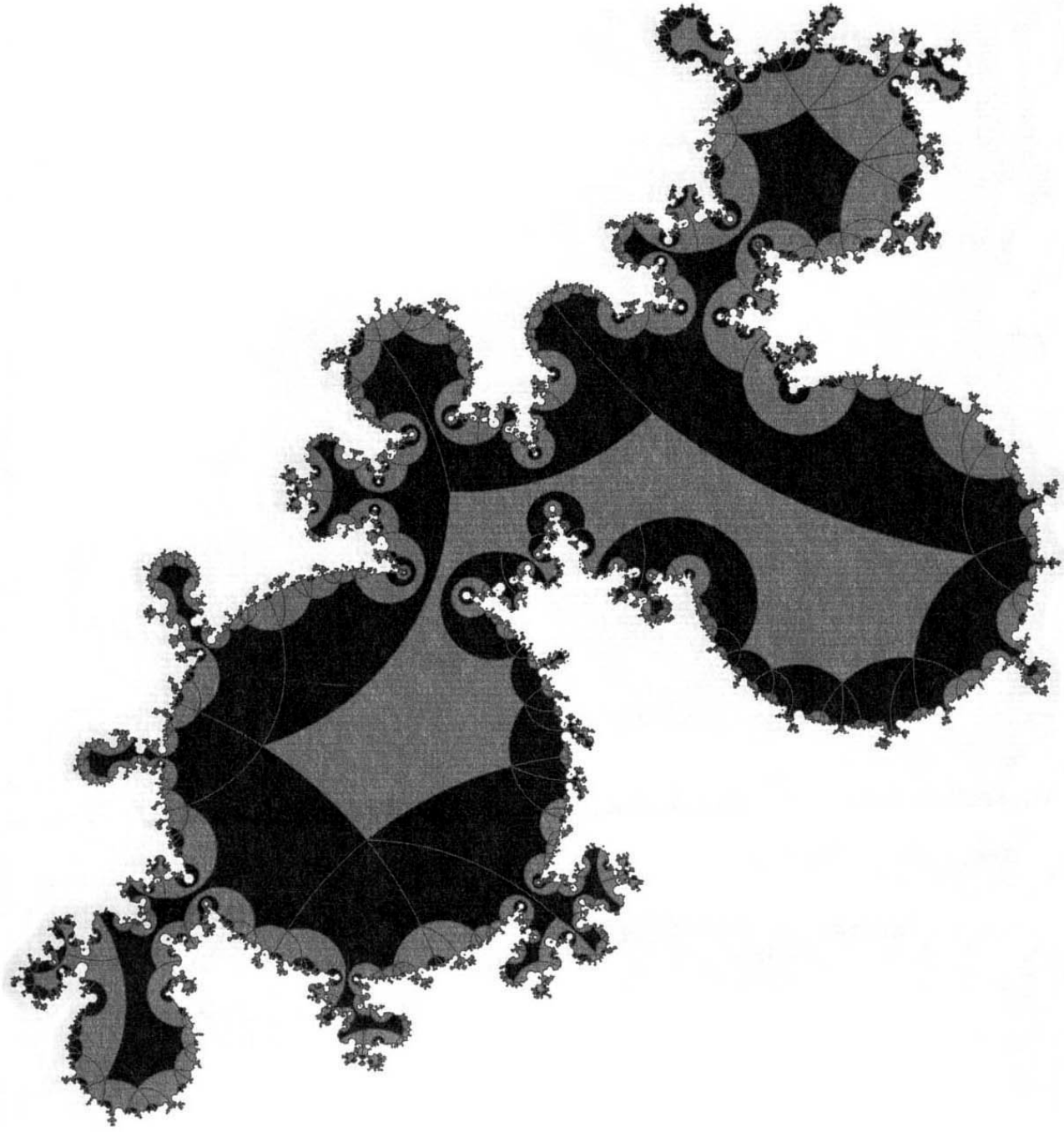

Fig.7

Figure 7: Same as figure 5, but for a manifold with the topology of figure 1 and the identification pattern in figure 2. This cluster is obviously quasi-self-similar; see the caption of figure 6. $\delta = 1.319$.

3. The ground state wave function (non-relativistic case)

The eigenvalue problem of the Schrödinger operator on the manifold is to solve (see [17])

$$\frac{-\hbar^2}{2m}\left[\Delta_{B^3} + \frac{1}{R^2}\right] u = E\, u, \tag{3.1}$$

where Δ_{B^3} is the Laplace-Beltrami operator on B^3,

$$\Delta_{B^3} := \frac{1}{4}\left(1 - \frac{r^2}{R^2}\right)^2 \left[\Delta_{E^3} + \frac{1}{R^2}\frac{2}{1-(r^2/R^2)} r\frac{\partial}{\partial r}\right],$$

and u is subject to periodic boundary conditions on the polyhedral faces. Thus u is automorphic under the Kleinian group Γ, satisfying in B^3 $u(\gamma\cdot) =$

$u(\cdot)$ for all $\gamma \in \Gamma$. The bound states are square-integrable in F with respect to the hyperbolic volume element $dV_{B^3} = 8(1 - |\mathbf{x}|^2/R^2)^{-3}dx^3$.

In (3.1) we have replaced the Laplace operator Δ_{E^3} in the free Euclidean Schrödinger equation by Δ_{B^3} and added a constant $1/R^2$,

$$-i\frac{\partial}{\partial t}\psi = \frac{\hbar}{2m}[\Delta_{B^3} + 1/R^2]\psi, \qquad \psi = u\exp(-iEt/\hbar), \tag{3.2}$$

so that the zero point of the energy scale lies at the bottom of the continuous spectrum. There is a unique bound state, the ground state, and an absolutely continuous spectrum in $[0, \infty]$. In [14] the connection between the ground-state energy and the Hausdorff dimension δ of $\Lambda(\Gamma)$ was derived by realizing that the convergence abscissa of the Poincaré series

$$\sum_{\gamma\in\Gamma}\left(1 - \frac{|\gamma\mathbf{x}|^2}{R^2}\right)^s \tag{3.3}$$

is the first pole of the Green's function of the operator $\Delta_{B^3} + 1/R^{-3}$, and thus the ground state of (3.1). The terms $(1 - (|\gamma\mathbf{x}|^2/R^2))$ in (3.3) can be interpreted for any fixed $\mathbf{x}$ as the radii $\mathbf{r}_\gamma$ of a Hausdorff cover of the limit set $\Lambda(\Gamma)$, which establishes the relation between the Hausdorff dimension δ and the first pole of the Green's function, the ground-state energy $E = (-\hbar^2/2mR^2)(\delta - 1)^2$. The analytic function defined by (3.3) has a first-order pole at $s = \delta$ on the convergence abscissa.

To construct the ground-state wave function of (3.1) we need explicit formulas for the absolute value and the Jacobi determinant of a transformation γ acting on B^3 (see [2]). Defining $[\mathbf{x}, \mathbf{y}] = (1 + |\mathbf{x}|^2\,|\mathbf{y}|^2 - 2\mathbf{x}\cdot\mathbf{y})^{1/2}$, $\mathbf{y} := \gamma^{-1}(\mathbf{0})$, and $\mathbf{0}$ the center of B^3, we have for the absolute value

$$|\gamma\mathbf{x}| = \frac{|\mathbf{x} - \mathbf{y}|}{[\mathbf{x}/R, \mathbf{y}/R]}, \tag{3.4}$$

and for the conformal dilatation

$$|\gamma'\mathbf{x}| = \frac{1 - |\mathbf{y}|^2/R^2}{[\mathbf{x}/R, \mathbf{y}/R]^2}, \tag{3.5}$$

where $|\gamma'\mathbf{x}|^3$ is the Jacobi determinant. Equation (3.4) can be written as

$$1 - \frac{|\gamma\mathbf{x}|^2}{R^2} = \frac{(1 - |\mathbf{x}|^2/R^2)(1 - |\mathbf{y}|^2/R^2)}{[\mathbf{x}/R, \mathbf{y}/R]^2}, \tag{3.6}$$

and the invariance of the B^3 line element under γ follows from

$$\frac{|\gamma'\mathbf{x}|}{1 - |\gamma\mathbf{x}|^2/R^2} = \frac{1}{1 - |\mathbf{x}|^2/R^2}. \tag{3.7}$$

Finally, $|\mathbf{x} - \mathbf{y}|/[\mathbf{x}/R, \mathbf{y}/R]$ is a point-pair invariant,

$$\frac{|\beta\mathbf{x} - \beta\mathbf{y}|}{[\beta\mathbf{x}/R, \beta\mathbf{y}/R]} = \frac{|\mathbf{x} - \mathbf{y}|}{[\mathbf{x}/R, \mathbf{y}/R]}, \tag{3.8}$$

for all $\mathbf{x},\mathbf{y}\in B^3$ and $\beta\in\Gamma$; and (3.5) satisfies

$$\frac{1-|\beta\mathbf{y}|^2/R^2}{[\beta\mathbf{x}/R,\beta\mathbf{y}/R]^2}|\beta'\mathbf{x}|=\frac{1-|\mathbf{y}|^2/R^2}{[\mathbf{x}/R,\mathbf{y}/R]^2}, \tag{3.9}$$

again for all $\mathbf{x},\mathbf{y}\in B^3$ and $\beta\in\Gamma$.

With formulas (3.4) and (3.5) one can decouple $\mathbf{x}$ from γ, expressing $|\gamma\mathbf{x}|$ and $|\gamma'\mathbf{x}|$ as functions of $\mathbf{x}$ and $\mathbf{y}:=\gamma^{-1}(\mathbf{0})$ alone.

Applying (3.6) we write the residue of (3.3) at $s=\delta$ as (see [14])

$$\begin{aligned}&\lim_{s\to\delta}(s-\delta)\sum_{\gamma\in\Gamma}\left(1-\frac{|\gamma\mathbf{x}|^2}{R^2}\right)^s\\&=\lim_{s\to\delta}(s-\delta)\sum_{\gamma\in\Gamma}\frac{(1-|\gamma\mathbf{0}|^2/R^2)^s(1-|\mathbf{x}|^2/R^2)^s}{[\mathbf{x}/R,\gamma\mathbf{0}/R]^{2s}}\\&=\lim_{s\to\delta}\int_{B^3}\frac{(1-|\mathbf{x}|^2/R^2)^s}{[\mathbf{x}/R,\boldsymbol{\eta}/R]^{2s}}(s-\delta)\sum_{\gamma\in\Gamma}(1-|\gamma\mathbf{0}|^2/R^2)^s\delta(\boldsymbol{\eta}-\gamma\mathbf{0})d\boldsymbol{\eta}\\&=\int_{B^3}\frac{(1-|\mathbf{x}|^2/R^2)^\delta}{[\mathbf{x}/R,\boldsymbol{\eta}/R]^{2\delta}}d\mu(\boldsymbol{\eta})=:u(\mathbf{x}),\quad\psi(\mathbf{x},t)=u(\mathbf{x})\exp(-iEt/\hbar)\end{aligned} \tag{3.10}$$

with

$$d\mu(\boldsymbol{\eta})=\lim_{s\to\delta}(s-\delta)\sum_{\gamma\in\Gamma}(1-|\gamma\mathbf{0}|^2/R^2)^s\delta(\boldsymbol{\eta}-\gamma\mathbf{0})d\boldsymbol{\eta} \tag{3.11}$$

Because $s\to\delta$, $d\mu(\boldsymbol{\eta})$ is supported only on the accumulation points of the supports $\gamma\mathbf{0}$ of the δ functions in (3.11), that is, on the limit set $\Lambda(\Gamma)$ on S_∞. Thus we can replace B^3 in the second integral in (3.10) by $\Lambda(\Gamma)$.

$u(\mathbf{x})$ defined in (3.10) is periodic (automorphic) with respect to Γ, $u(g\cdot)=u(\cdot)$, $g\in\Gamma$. This follows from (3.9) and the transformation property

$$d\mu(g\boldsymbol{\eta})=|g'\boldsymbol{\eta}|^\delta d\mu(\boldsymbol{\eta}) \tag{3.12}$$

of $d\mu$, which is readily derived by applying to (3.11) successively $\delta(g\boldsymbol{\eta}-\gamma\mathbf{0})d(g\boldsymbol{\eta})=\delta(\boldsymbol{\eta}-g^{-1}\gamma\mathbf{0})d\boldsymbol{\eta}$, formula (3.7), and $|(g^{-1})'|=|g'|^{-1}$.

The geometric meaning of the conformal dilatation (3.5) is this: an infinitesimal ball B centered at $\boldsymbol{\eta}$ with Euclidean radius ε is transformed by g into a ball $g(\mathrm{B})$ with radius $\varepsilon|g'\boldsymbol{\eta}|$. This extends also to disks on S_∞. Since $|g'\boldsymbol{\eta}|$ is the change of scale and δ is the Hausdorff dimension, $d\mu$ measures the volume of sufficiently small disks of radius r centered at $\Lambda(\Gamma)$, like r^δ; $d\mu$ is the Hausdorff measure of $\Lambda(\Gamma)$.

Finally, because the last integral in (3.10) is supported only on S_∞, we can replace $[\mathbf{x}/R,\boldsymbol{\eta}/R]$ by $|\mathbf{x}-\boldsymbol{\eta}|/R$. The Poisson kernel $(1-|\mathbf{x}|^2/R^2)/|\mathbf{x}-\boldsymbol{\eta}|^2$ satisfies in B^3

$$\left[\frac{-\hbar^2}{2m}(\Delta_{B^3}+1/R^2)-E(\delta)\right]\left[\frac{1-|\mathbf{x}|^2/R^2}{|\mathbf{x}-\boldsymbol{\eta}|^2}\right]^\delta=0 \tag{3.13}$$

if $|\boldsymbol{\eta}| = R$ and $E(\delta) = (-\hbar^2/2mR^2)(\delta - 1)^2$. Thus we have the following Helgason representation [6] of the ground-state wave function:

$$\psi(\mathbf{x}, t) = \exp\left(\frac{i\hbar(\delta-1)^2 t}{2mR^2}\right) \int_{\Lambda(\Gamma)} \frac{(1 - |\mathbf{x}|^2/R^2)^\delta}{|\mathbf{x} - \boldsymbol{\eta}|^{2\delta}} d\mu(\boldsymbol{\eta}) \tag{3.14}$$

The function is square-integrable for $1 < \delta < 2$. (Our manifolds have infinite volume, therefore the case $\delta = 2$ cannot occur. If $\delta \to 1$ then $E(\delta)$ moves toward the lower edge of the continuous spectrum. If $\delta = 1$ there is no bound state, and the convex hull of the limit set (see section 2) degenerates to a spherical cap.)

This function is completely determined by the limit set $\Lambda(\Gamma)$ and by its Hausdorff dimension and measure. On the other hand, Λ can be obtained by lifting the bounded trajectories into the covering space of the manifold; the initial and end points of these lifts constitute $\Lambda(\Gamma)$. This is the reconstruction of the bound-state wave function in terms of the bounded chaotic trajectories discussed in the introduction.

4. Isothermal coordinates at infinity of hyperbolic space and the emergence of the limit set

The limit set $\Lambda(\Gamma)$ determines the bounded trajectories as well as the support of the Hausdorff measure in the integral representation of the ground-state wave function, and in this section we will look at it more closely.

We start with a manifold that has a principal-circle group Γ as a group of covering transformations; the limit set $\Lambda(\Gamma)$ is then a circle. We project S_∞ stereographically onto the extended complex plane. A Riemannian metric on f_1 (see figure 2) is then of the form

$$ds^2 = E\,dx^2 + 2F\,dx\,dy + G\,dy^2 = \lambda^2(z, \bar{z})\,|dz + \mu(z, \bar{z}) d\bar{z}|^2; \tag{4.1}$$

in the following we will suppress the conjugated variable in λ and μ.

Since $EG - F^2 > 0$, $E > 0$, and f_1 is a compact surface, we have $|\mu(z)| \leq K < 1$, $\lambda > 0$ on f_1.

Γ acts on $\mathbb{C}$ as a discrete group of Möbius transformations

$$z \to (az + b)/(cz + d), \qquad \begin{pmatrix} a & b \\ c & d \end{pmatrix} \in SL(2, \mathbb{C}).$$

Conjugating Γ with an appropriate Möbius transformation, we may assume that the projected limit set is just the unit circle, so that $\Gamma(f_1)$ tesselates the interior and $\Gamma(f_2)$ the exterior of the unit disk U.

In order that ds^2 fit smoothly on the identified boundaries of f_1 it must be invariant under Γ. We have

$$\begin{aligned} &\lambda^2(g(z))\,|dg(z) + \mu(g(z))\overline{dg(z)}|^2 \\ &\quad = \lambda^2(g(z))\,|g_z(z)|^2 \left| dz + \mu(g(z))\frac{\overline{g_z}}{g_z} d\bar{z} \right|^2 \end{aligned} \tag{4.2}$$

where g_z denotes the derivative. Thus, if we extend λ and μ to U by requiring

$$\lambda^2(g(z)) = \lambda^2(z)\frac{1}{g_z\overline{g_z}} \tag{4.3}$$

and

$$\mu(g(z)) = \mu(z)\frac{g_z}{\overline{g_z}}, \tag{4.4}$$

for example, $\mu = 0$, $\lambda = (1-|z|^2)^{-1}$, then the invariance of ds^2 follows.

The space of functions μ that satisfy in U $|\mu| \leq K < 1$ and (4.4) can be parametrized by $6(g-1)$ independent complex parameters, g being the genus of f_1. This follows from the Riemann-Roch theorem, for μ can be represented as $\mu = (1-|z|^2)^2\overline{\varphi(z)}$, where $\varphi(z)$ is a bounded quadratic differential, $\varphi(g(z))g_z^2 = \varphi(z)$ for $g \in \Gamma$, and $|\varphi(z)| < \text{const.}(1-|z|^2)^{-2}$ in U.

There is a standard way to generate such differentials and thus uniformly bounded μ with the property (4.4), namely by the Poincaré series

$$\overline{\mu(z)} = (1-|z|^2)^2 \sum_{g\in\Gamma} h(g(z))g_z^2, \tag{4.5}$$

where h is an analytic function in U such that $\int_U |h|(1-|z|^2)^{-2}dz < \infty$.

A deformation of the manifold via contractions and dilatations along its necks corresponds now to the introduction of global isothermal coordinates on f_1 (or f_2) for a given metric determined by a μ and a λ that fulfill (4.3) and (4.4).

We ask for a diffeomorphism $z \to \omega(z)$ that makes ds in (4.1) proportional to the Euclidean line element:

$$ds = \lambda(z)\,|dz + \mu(z)d\overline{z}| = C(\omega)\,|d\omega|, \tag{4.6}$$

where $C(\omega)$ is an arbitrary proportionality factor. We have from (4.6)

$$ds = C(\omega(z))\,|\omega_z|\left|dz + \frac{\omega_{\overline{z}}}{\omega_z}d\overline{z}\right|, \tag{4.7}$$

where $\omega_{\overline{z}}$ is the derivative with respect to the conjugated variable; thus ω is a solution of the Beltrami equation (see [1])

$$\omega_{\overline{z}} = \mu\omega_z. \tag{4.8}$$

We extend μ to all of $\mathbb{C}$ by requiring $\mu \equiv 0$ (i.e., ω analytic) outside the unit disk U. Then there exists a homeomorphism $\mathbb{C} \to \mathbb{C}$, $z \to \omega(z)$ that is differentiable in U, analytic for $|z| > 1$, and satisfies equation (4.8) in $\mathbb{C}$, with the exception of the unit circle S where μ is discontinuous.

Since ω is non-differentiable on the unit circle, it maps S onto a fractal curve (homeomorphically). Moreover, it is determined up to a Möbius transformation, and $\omega\Gamma\omega^{-1}$ is again a group of Möbius transformations. This follows from (4.4), the chain rule (see [1])

$$\mu_{g\circ f^{-1}}(f(z)) = \frac{\mu_g(z)-\mu_f(z)}{1-\overline{\mu_f(z)}\mu_g(z)}\frac{f_z(z)}{\overline{f_z(z)}} \tag{4.9}$$

where $\mu_f := f_{\bar{z}}/f_z$, and the fact that the only meromorphic invertible functions in the extended complex plane are Möbius transformations.

ω can be constructed explicitly via an integral equation equivalent to (4.8). Since $\omega(z)$ is determined only up to a Möbius transformation, we fix it by requiring $\omega(z) \to z$ for $|z| \to \infty$. Applying the generalized Cauchy formula for non-analytic functions (see [1]) to $\omega(z) - z$ gives

$$\omega(z) = z - \frac{1}{\pi}\int_U \frac{\omega_{\bar{z}}(\zeta)}{\zeta - z} d\zeta. \tag{4.10}$$

Differentiating (4.10) and using (4.8) we have

$$\omega_{\bar{z}}(z) = \mu(z)\left[1 - \frac{1}{\pi}\int_U \frac{\omega_{\bar{z}}(\zeta)}{(\zeta - z)^2} d\zeta\right]. \tag{4.11}$$

The standard iteration procedure for (4.11) gives finally ($\mu(z) \leq K < 1$)

$$\omega_{\bar{z}}(z) = \mu(z)\Bigg[1 - \frac{1}{\pi}\int_U \frac{\mu(\zeta_1)}{(\zeta_1 - z)^2} d\zeta_1 + \frac{1}{\pi^2}\int_U\int_U \frac{\mu(\zeta_1)\mu(\zeta_2)}{(\zeta_1 - \zeta_2)^2(\zeta_2 - z)^2} d\zeta_1\, d\zeta_2 - \cdots\Bigg] \tag{4.12}$$

Applying the homeomorphism $\omega(z)$ of the complex plane constructed via (4.5), (4.12), and (4.10) to the unit circle, we get limit sets as depicted in figures 4 through 7.

5. Open Robertson-Walker cosmologies of multiple connectivity

We consider cosmological line elements of the form

$$ds^2 = -c^2 dt^2 + a^2(t) d\sigma^2, \tag{5.1}$$

where $d\sigma^2$ is the metric of hyperbolic 3-space, which we may represent in the coordinates (2.1) of the Poincaré ball B^3 .The expansion factor of 3-space $a(t)$ determines the Gaussian curvature $K = -1/(aR)^2$ of the space-like sections $t =$ constant. The space-like projections of the geodesics into B^3 calculated via (5.1) are, as in the non-relativistic case, arcs of semicircles orthogonal to S_∞. Only the time dependence of the geodesics changes (see [18]).

The topological structure of 4-space is now $\mathbb{R}^+ \times I \times S$, $\mathbb{R}^+$ being the time axis $0 < t < \infty$, and the 3-space $I \times S$ (I a finite open interval, S a compact Riemann surface) is again represented in B^3 as a polyhedron F with face-identification by Γ. We mention that F and Γ can also vary in time, constituting a one-parameter family $(F(t), \Gamma(t))$ of non-isometric 3-manifolds. Even the topological structure of 3-space may change; for example, it could disintegrate by developing parabolic cusp singularities at the boundary of the deformation space (see [3, 7]).

We call a trajectory bounded if it stays in a finite region that is not expanding faster than 3-space itself . The bounded chaotic trajectories are

again intimately connected with the limit set $\Lambda(\Gamma)$. For example, if the expansion factor $a(t)$ is of the order t^α, $\alpha \geq 1$ for $t \to 0$, a trajectory is then bounded for $t \to 0$ only if its lifts in the covering space emanate from $\Lambda(\Gamma)$; in this case it has the Bernoulli property. Likewise, if $a(t)$ is of order t^β, $\beta \leq 1/2$ for $t \to \infty$, it is then bounded for $t \to \infty$ only if its lifts end in the limit set $\Lambda(\Gamma)$. In de Sitter space ($a(t) = \sinh(\Lambda t)$) the bounded trajectories are exactly those that emanate from $\Lambda(\Gamma)$ (see [18]).

The wave equation on the covering space $\mathbb{R}^+ \times B^3$ reads

$$\left[\Box - \xi\hat{R} - (mc/\hbar)^2\right]\psi = 0, \tag{5.2}$$

where $\Box$ is the Laplace-Beltrami operator of the line element ds^2 in $\mathbb{R}^+ \times B^3$ ($\Box\psi := g^{\alpha\beta}\psi_{;\alpha\beta}$), and ξ is the (dimensionless) coupling to the curvature scalar $\hat{R}$. Imposing as in section 3 Γ-periodic boundary conditions on ψ, we get the wave equation on the manifold $\mathbb{R}^+ \times I \times S$.

Separation of variables $\psi(t, \mathbf{x}) = \hat{\psi}(\mathbf{x})\varphi(t)$ in (5.2) gives

$$\left[\Delta_{B^3} + R^{-2}\delta(2-\delta)\right]\hat{\psi} = 0, \tag{5.3}$$

where Δ_{B^3} is the Laplace-Beltrami operator of B^3 as in (3.1), and the separation constant $R^{-2}\delta(2-\delta)$ appears as a spectral parameter. Here we keep (F, Γ) independent of time, otherwise equation (5.2) is not separable. For φ we have

$$\ddot{\varphi} + 3\frac{\dot{a}(t)}{a(t)}\dot{\varphi} + \left[(mc^2/\hbar)^2 + \Lambda^2\delta(2-\delta)a^{-2}(t) + c^2\xi\hat{R}(t)\right]\varphi = 0, \tag{5.4}$$

with $\Lambda = c/R$.

Concerning the time dependence of ψ, we impose the following end-value condition on $\varphi(t)$ (positive frequency solutions): $\varphi(t) \sim f(t)e^{-ig(t)}$ for $t \to \infty$, with real f, g; $f(t)$ monotonically decreasing; and $g(t)$ strictly monotonically increasing, thus approximating as well as possible the Minkowski space solutions in the asymptotic regime, when 3-space gets flat.

Equation (5.3) we discussed in section 3: there is a unique bound state for a δ in the open interval $(1, 2)$, and absolutely continuous spectrum for $\delta(2-\delta) \geq 1$.

With the covariant and indefinite scalar product for wave fields as in [18], the normalization condition for φ reads

$$\frac{1}{2}\left(\dot{\overline{\varphi}}\varphi - \dot{\varphi}\overline{\varphi}\right) = \pm i\, a^{-3}(t), \tag{5.5}$$

where $\varphi, \overline{\varphi}$ is a pair of fundamental solutions of (5.4).

The energy-momentum tensor $T_{\mu\nu}$ of the field in (5.2) we get by variation of the action functional

$$S = \int dx^4\sqrt{-g}\left\{\frac{1}{2}g^{\mu\nu}\left[\psi_{,\mu}\overline{\psi}_{,\nu} + \overline{\psi}_{,\mu}\psi_{,\nu}\right] + \left[(mc/\hbar)^2 + \xi\hat{R}\right]\psi\overline{\psi}\right\} \tag{5.6}$$

with respect to the metric $g^{\mu\nu} \to g^{\mu\nu} + \delta g^{\mu\nu}$:

$$\delta S = \int dx^4 \sqrt{-g}\, \delta g^{\mu\nu} T_{\mu\nu}. \tag{5.7}$$

For the calculation of $T_{\mu\nu}$ we need the variation of the determinant, $\delta g = -g g_{\mu\nu} \delta g^{\mu\nu}$, and the variation of the Ricci tensor, $g^{\mu\nu}\delta\hat{R}_{\mu\nu} = \omega^{\lambda}{}_{,\lambda}$, with $\omega^{\lambda} = g^{\mu\nu}\delta\Gamma^{\lambda}_{\mu\nu} - g^{\mu\lambda}\delta\Gamma^{\nu}_{\mu\nu}$ (we use locally geodesic coordinates, $\Gamma^{\alpha}_{\beta\gamma} = 0$, $g_{\mu\nu,\lambda} = 0$, and the sign conventions of reference [13]). Expressing $\Gamma^{\nu}_{\mu\nu}$ and $g^{\mu\nu}\Gamma^{\lambda}_{\mu\nu}$ in terms of g, $g^{\mu\nu}$, and their derivatives (see [4, 12]), we arrive finally at $\omega^{\lambda} = -\delta g^{\lambda\mu}{}_{,\mu} + g^{\kappa\lambda} g_{\mu\nu} \delta g^{\mu\nu}{}_{,\kappa}$. By applying Green's theorem in locally geodesic coordinates, and then passing over to covariant derivatives, we obtain the energy-momentum tensor of a scalar field coupled to the Ricci scalar:

$$T_{\mu\nu} = t^{(\mathrm{min.})}_{\mu\nu} + \xi t^{(\mathrm{ext.})}_{\mu\nu}, \tag{5.8}$$

with

$$t^{(\mathrm{min.})}_{\mu\nu} = \frac{1}{2}\left(\psi_{,\mu}\overline{\psi_{,\nu}} + \mathrm{c.c.}\right) - \frac{1}{4} g_{\mu\nu} g^{\alpha\beta}\left(\psi_{,\alpha}\overline{\psi_{,\beta}} + \mathrm{c.c.}\right) - \frac{1}{2}(mc/\hbar)^2 \psi\overline{\psi} g_{\mu\nu}$$

and

$$\begin{aligned} t^{(\mathrm{ext.})}_{\mu\nu} = {} & \left(\hat{R}_{\mu\nu} - \frac{1}{2}\hat{R} g_{\mu\nu}\right)\psi\overline{\psi} - \left(\psi_{,\mu}\overline{\psi_{,\nu}} + \overline{\psi}\psi_{;\mu\nu} + \mathrm{c.c.}\right) \\ & + g_{\mu\nu} g^{\alpha\beta}\left(\psi_{,\alpha}\overline{\psi_{,\beta}} + \overline{\psi}\psi_{;\alpha\beta} + \mathrm{c.c.}\right). \end{aligned}$$

For the calculation of T_{00} we note that $\psi_{;00} = \psi_{,00}$ (because the relevant 3-indices vanish), and we eliminate $\psi_{;\alpha\beta}$ in (5.8) by means of the wave equation (5.2). Finally, $\hat{R}_{00} = -3\ddot{a}/a$, and

$$\hat{R} = 6\left[\frac{-1}{a^2(t)R^2} + \frac{\ddot{a}(t)}{c^2 a(t)} + \frac{\dot{a}^2(t)}{c^2 a^2(t)}\right]. \tag{5.9}$$

The energy of the wave field is calculated as

$$E = \hbar c^2 \int_{\Sigma} T_{0\mu} d\Sigma^{\mu}, \tag{5.10}$$

with Σ an arbitrary space-like hypersurface for which we may choose the 3-space. Then Σ^0 is the only non-vanishing component of $d\Sigma^{\mu}$, and is given by $d\Sigma^0 = a^3(t) dV_{B^3}$, where dV_{B^3} is the volume element of (2.1).

Applying Green's formula again in (5.10), we arrive finally at

$$\begin{aligned} E(t,\delta) = \frac{1}{2}\hbar a^3 \Bigg\{ & \left(\varphi_{,t} + 6\xi\varphi\frac{\dot{a}}{a}\right)\overline{\left(\varphi_{,t} + 6\xi\varphi\frac{\dot{a}}{a}\right)} \\ & + \varphi\overline{\varphi}\left[\left(\frac{mc^2}{\hbar}\right)^2 + \Lambda^2\left[\delta\left(2-\delta\right) - 6\xi\right]a^{-2} + 6\xi(1-6\xi)\frac{\dot{a}^2}{a^2}\right]\Bigg\}, \end{aligned} \tag{5.11}$$

which generalizes the energy formula in [18] to the non-minimally coupled case, which is as we will soon see essential for the treatment of massless particles. Note that (5.11) no longer contains the space part of the wave field. This expression is obviously positive definite for $0 \leq 6\xi \leq \min[1, \delta(2-\delta)]$; but positivity is too restrictive a condition, for example in the treatment of massless particles. What we will require is uniform boundedness of the energy functional from below.

We discuss (5.11) valid for every Robertson-Walker line element in the context of de Sitter space. We then have $a(t) = \sinh(\Lambda t)$, where $3\Lambda^2/c^2$ is the cosmological constant, $\hat{R} = 12\Lambda^2/c^2$, and $R = c/\Lambda$. We define

$$\kappa^2 = -\frac{1}{4} - 2(1-6\xi) + \left(\frac{mc^2}{\hbar\Lambda}\right)^2 \quad \text{and} \quad \nu^2 = 1 - \delta(2-\delta), \tag{5.12}$$

and assume $\kappa^2 > 0$ to ensure the right time behavior at infinity. The positive frequency solution for $t \to \infty$ is then

$$\begin{aligned}\varphi(t) = {} & (\Lambda|\kappa|)^{-1/2} 2^{(3/2+i\kappa)} e^{-\Lambda t(3/2+i\kappa)} \\ & \times \left\{1 + \frac{e^{-2\Lambda t}}{1+i\kappa}\left[\frac{5}{4} + \nu^2 + \frac{3}{2}i\kappa\right] + O(e^{-4\Lambda t})\right\},\end{aligned} \tag{5.13}$$

and for $t \to 0$, $\nu > 0$ (ground state),

$$\varphi_{\text{g.st.}}(t) \sim \frac{2^{i\kappa}}{\sqrt{2\pi|\kappa|\Lambda}} \frac{\Gamma(1+i\kappa)\Gamma(\nu)2^{\nu}}{\Gamma(1/2+i\kappa+\nu)} (\Lambda t)^{-\nu-1}. \tag{5.14}$$

For $t \to 0$, $\mathrm{Im}(\nu) > 0$ (continuous spectrum),

$$\begin{aligned}\varphi(t) \sim {} & \frac{2^{i\kappa}\Gamma(1+i\kappa)}{\sqrt{2\pi|\kappa|\Lambda}} \\ & \times \left[\frac{\Gamma(-\nu)2^{-\nu}}{\Gamma(1/2+i\kappa-\nu)}(\Lambda t)^{\nu-1} + \frac{\Gamma(\nu)2^{\nu}}{\Gamma(1/2+i\kappa+\nu)}(\Lambda t)^{-\nu-1}\right].\end{aligned} \tag{5.15}$$

The negative frequency solutions are conjugated to them.

With these solutions we obtain the time evolution of energy in the asymptotically flat region,

$$E(t \to \infty, m > 0) \sim \frac{m^2c^4}{\hbar\Lambda|\kappa|} = mc^2 + O(\hbar^2), \tag{5.16}$$

and

$$E(t \to \infty, m = 0) \sim \frac{2\hbar\Lambda(1-6\xi)[36\xi - 5\delta(2-\delta)]}{\sqrt{12\xi - 9/4}\,(12\xi - 5/4)} e^{-2\Lambda t}. \tag{5.17}$$

The leading order of the asymptotic expansion is independent of the spectral variable ν.

At the beginning of the evolution, for $t \to 0$, we have

$$E(\nu > 0, t \to 0) \sim \frac{\hbar \Lambda 2^{2\nu-1}\Gamma^2(\nu)(1+\nu)(1-6\xi)}{\sinh(\pi|\kappa|)|\Gamma(1/2+\nu+i\kappa)|^2}(\Lambda t)^{-2\nu-1}. \tag{5.18}$$

Finally, for $\mathrm{Im}(\nu) > 0$, writing $\nu = i\tilde{\nu}$, $\tilde{\nu} = \sqrt{\delta(2-\delta)-1} > 0$,

$$E(\mathrm{Im}(\nu) = \tilde{\nu} > 0, t \to 0) \sim \frac{\hbar}{t}\left\{A(\tilde{\nu},\kappa,\xi) + \mathrm{Re}\left[B(\tilde{\nu},\kappa,\xi)(\Lambda t)^{2i\tilde{\nu}}\right]\right\}, \tag{5.19}$$

with

$$A(\tilde{\nu},\kappa,\xi) = \tilde{\nu}^{-1}\coth(\pi|\kappa|)\coth(\pi\tilde{\nu})(\tilde{\nu}^2+1-6\xi)$$

and

$$B(\tilde{\nu},\kappa,\xi) = \frac{(1-6\xi)(1-i\tilde{\nu})}{\sinh(\pi|\kappa|)}\frac{\Gamma^2(-i\tilde{\nu})2^{-2i\tilde{\nu}}}{\Gamma(1/2-i\tilde{\nu}+i\kappa)\Gamma(1/2-i\tilde{\nu}-i\kappa)}.$$

In the initial state of the cosmic expansion (for $t \to 0$), there is an infinite oscillation of E (equation (5.19)) between the two curves $\hbar t^{-1}(A \pm |B|)$ with an amplitude $\hbar t^{-1}|B|$ and a frequency $(e^{\pi/\tilde{\nu}}-1)^{-1}t^{-1}$, both diverging to infinity ($A - |B| > 0$; see below). On the other hand, the energy associated with the discrete eigenvalue (equation (5.18), and $1 - 6\xi > 0$) does not fluctuate at all, and overpowers that of the continuous spectrum (see equation (5.19)) for any fixed $\tilde{\nu}$. However, we see from the following asymptotic expansion,

$$E(\tilde{\nu} \to \infty, t) = \frac{\hbar\Lambda}{a(t)}\tilde{\nu}\left[1 + O(1/\tilde{\nu}^2)\right], \tag{5.20}$$

valid for any fixed t, that it lies well inside the range of energies obtainable from the continuous spectrum. We compare these formulas with the classical energy, $E = mc^2\sqrt{1 + \text{const.}\, a^{-2}(t)}$. The constant depends on the initial velocity, and E does not depend at all on the trajectory, bounded and chaotic or regular and unbounded. The only thing that is common to the classical and quantum energies is the inverse time behavior ($a^{-1}(t)$) for $t \to 0$.

Finally we discuss the boundedness of E. Every solution of (5.2) depends on three parameters: m, ξ, and the spectral variable $\delta(2-\delta)$. There are restrictions on m and ξ: $\kappa^2(m,\xi)$ in equation (5.12) must be positive in order to fulfill the boundary conditions. The requirement on E of uniform boundedness from below, simultaneously for t and $\delta(2-\delta)$ for fixed m and ξ, imposes further restrictions on the spectral variable $\delta(2-\delta)$. At first we note that, in equation (5.18), we have to require $1 - 6\xi > 0$. If this is not satisfied we exclude the solution corresponding to the discrete eigenvalue, as is the case for $m = 0$. The smallest value that the second term in (5.19)

periodically admits is $-|B|$. The necessary and sufficient condition that ensures boundedness of E from below for $t \to 0$ is thus $A - |B| > 0$, or

$$F(\tilde{\nu}) := \tilde{\nu}^2 + 1 - 6\xi - \sqrt{\tilde{\nu}^2+1}\,|1-6\xi|\,\frac{1}{\cosh(\pi\kappa)}\sqrt{1+\frac{\sinh^2(\pi\kappa)}{\cosh^2(\pi\tilde{\nu})}} > 0, \tag{5.21}$$

with $0 < \tilde{\nu} < \infty$ and $\tilde{\nu} = \sqrt{\delta(2-\delta)-1}$. Note that $F(\tilde{\nu}) = 1 - 6\xi - |1-6\xi| + O(\tilde{\nu}^2)$. There is for given m and ξ at most a finite interval to be excluded from the spectrum of Δ_{B^3} to ensure $E(\nu,t) > \text{const.}(m,\xi)$ for $t \to 0$. From the asymptotic formulas (5.16), (5.17), and (5.20), and from the asymptotic behavior of the exact solution [18] for $\tilde{\nu} \approx \text{const.}\exp(\Lambda t) \to \infty$ ($|\varphi(\tilde{\nu},t)| \approx \text{const.}\exp(-3/2\,\Lambda t)$, which gives a lower bound for the second term in (5.11)), we conclude that the energy functional is bounded from below, uniformly for all t and ν with the exception of the excluded interval. It can be made positive definite by adding a finite constant, independent of ν and t.

6. Conclusions and outlook

We have given an example for the reconciliation of the concept of a wave function with that of classical trajectories in an unstable system, geodesic motion in infinite, constantly curved spaces of multiple connectivity. This interdependence of trajectories and wave functions is mediated in the universal covering space B^3 of the manifold by the limit set $\Lambda(\Gamma)$ of the Kleinian group Γ of covering transformations. This fractal point set at infinity of hyperbolic space comprises all the information that is contained in the wave function, which appears as the solution of a boundary value problem in B^3, with the boundary data provided by the Hausdorff measure on $\Lambda(\Gamma)$.

Three-manifolds of the above-mentioned type appear as space-like sections in Robertson-Walker cosmologies. Their multiple connectivity produces chaotic trajectories and bound states (square-integrable chaotic wave fields), which are determined by the limit sets of the covering groups of the space-like slices. In section 5 we discussed in some detail in the context of de Sitter space the asymptotic time behavior of the energy of such wave fields, and its dependence on the Hausdorff dimension of the limit sets.

We considered scalar wave fields coupled to the Ricci scalar. This coupling by the dimensionless parameter ξ has no analogy in classical mechanics. The curvature scalar (5.9) of Robertson-Walker cosmologies depends only on the time variable, and may change its sign during the time evolution. Even in de Sitter space, where the Ricci scalar is a constant, it is not possible to absorb it in the mass term of equation (5.2), for this would lead to a different energy (see (5.11)). The reason for this is that, in (5.11), the variation of the Ricci scalar also enters. Thus, even in de Sitter space the energy depends in a non-trivial way on three parameters: ξ, m, and the spectral variable ν. It is again the energy functional that, for given m and ξ, determines the range

of the admissible values of the spectral variable by the condition of uniform boundedness (see (5.21)).

Finally a comment on the energy formulas (5.18) and (5.19). The bound state has a simple power law behavior that is more strongly singular than that of the extended states because of a localization phenomenon explained in [18]. Moreover, the extended states show oscillations with a frequency and an amplitude both diverging to infinity, so that the energy becomes ultimately unresolvable, lying in the band $\hbar t^{-1}(A \pm |B|)$, which indicates the instability of the extended states at the beginning of the expansion.

It was noted long ago [15] that a time-dependent expansion factor can cause backscattering of freely propagating classical fields, and may lead to production-annihilation processes in quantum fields. The point is that an initially more or less monochromatic wave packet can receive during its evolution admixtures of waves traveling in the opposite direction. In the classical case the situation is then similar to the wave propagation in a medium with a time-dependent index of refraction [10]. However, with a conformally coupled field like the electromagnetic one such effects cannot occur in a topologically trivial space, the evolution being equivalent to that in a static universe, modulo some rescaling with the expansion factor. A wave packet composed initially of positive frequencies will never develop negative ones. However, that is not true if 3-space is multiply connected. This comes as follows.

In the simply connected Robertson-Walker models the space-like sections at different instants of time are always isometric after rescaling with a constant factor. In the multiply connected models, though perfectly isotropic, the situation is quite different. Here the fundamental polyhedron embedded in hyperbolic space may itself vary in time; for example, the dihedral angles and the 3-manifolds that are obtained by imposing the Minkowski metric onto them are generically non-isometric (see section 5). In fact, a Robertson-Walker cosmology is determined by a time-dependent expansion factor and a time-dependent path in the deformation space of the polyhedron representing 3-space [3, 7]. A mixing of positive-negative frequencies can occur because of this second time dependence, even if the expansion factor does not vary or the field is conformally coupled.

Apart from the mixing of modes because of this time dependence, we have backscattering independent of time for classical fields just because of the high connectivity of 3-space, as we have it for classical trajectories. This topological scattering must be very irregular and chaotic, and the scattered wave trains will finally be uniformly distributed over the space manifold, which might provide a new explanation of the background radiation.

Acknowledgments

The author acknowledges the partial support of the European Communities through their Science Programme under grant B/SC1*-915078.

The numerical calculations were done in the I. Prigogine Center for Statistical Mechanics at the University of Texas; I thank Lea Vetter and Paul

Morris for their assistance with the graphics, and P. Kinet for the drawings. Finally I thank the Fondation Arp, Clamart, for permission to reproduce figure 1.

References

[1] L. V. Ahlfors, *Lectures on Quasiconformal Mappings* (New York, Van Nostrand, 1966).

[2] L. V. Ahlfors, "Möbius Transformations in Several Dimensions," lecture notes, University of Minnesota (1981).

[3] L. Bers, "On Boundaries of Teichmüller Spaces and on Kleinian Groups," *Annals of Mathematics*, **91** (1970) 570–600.

[4] N. D. Birrell and D. C. W. Davies, *Quantum Fields in Curved Space* (Cambridge, Cambridge Univ. Press, 1982).

[5] O. Heckmann and E. Schuecking, "Newtonian and Einsteinian Cosmology," *Handbuch der Physik*, **53** (1959) 489–519.

[6] S. Helgason, *Harmonic Analysis on Homogeneous Spaces* (Berlin, Birkhäuser, 1981).

[7] D. A. Hejhal, "Regular b-groups, Degenerating Riemann Surfaces, and Spectral Theory," *Memoirs of the AMS*, **88**(437) (1990).

[8] L. Infeld and A. Schild, "A New Approach to Kinematic Cosmology," *Physical Review*, **68** (1945) 250–272.

[9] S. L. Krushkal, B. N. Apanasov, and N. A. Grusevskii, "Kleinian Groups and Uniformization in Examples and Problems," *Translations of Mathematical Monographs*, **62** (Providence, RI, American Mathematical Society, 1986).

[10] L. D. Landau and E. M. Lifshitz, *The Classical Theory of Fields* (London, Pergamon, 1971).

[11] J. Lehner, *Discontinuous Groups and Automorphic Functions* (Providence, RI, American Mathematical Society, 1964).

[12] G. C. McVittie, *General Relativity and Cosmology* (London, Chapman and Hall, 1956).

[13] C. W. Misner, K. S. Thorne, and J. A. Wheeler, *Gravitation* (New York, Freeman, 1973).

[14] S. J. Patterson, "The Limit Set of a Fuchsian Group," *Acta Mathematica*, **136** (1976) 241–273.

[15] E. Schrödinger, "The Proper Vibrations of the Expanding Universe," *Physica*, **6** (1939) 899–912.

[16] W. Thurston, "The Geometry and Topology of 3-Manifolds," unpublished lecture notes, Princeton University (1978).

[17] R. Tomaschitz, "On the Calculation of Quantum Mechanical Ground States from Classical Geodesic Motion on Certain Spaces of Constant Negative Curvature," *Physica*, **D34** (1989) 42–89.

[18] R. Tomaschitz, "Relativistic Quantum Chaos in Robertson-Walker Cosmologies," *Journal of Mathematical Physics*, **32** (1991) 2571–2579.

[19] R. Tomaschitz, "An Alternative to Wave Mechanics on Curved Spaces," *International Journal of Theoretical Physics*, **31** (1992) 187–209.

[20] R. Tomaschitz, "Chaotic Dynamics in General Relativity," in *Chaotic Dynamics: Theory and Practice*, edited by T. Bountis (Plenum, NY, NATO-ASI series (1992).